

24. Zietkiewicz, E. *et al.* Genetic structure of the ancestral population of modern humans. *J. Mol. Evol.* **47**, 146–155 (1998).
25. Rogers, A. R. & Harpending, H. Population growth makes waves in the distribution of pairwise genetic differences. *Mol. Biol. Evol.* **9**, 552–569 (1992).
26. Fu, Y. X. & Li, W. H. Statistical tests of neutrality of mutations. *Genetics* **133**, 693–709 (1993).
27. Tajima, F. Statistical method for testing the neutral mutation hypothesis by DNA polymorphism. *Genetics* **123**, 585–595 (1989).
28. Rozas, J. & Rozas, R. DnaSP, DNA sequence polymorphism: an interactive program for estimating population genetics parameters from DNA sequence data. *Comput. Appl. Biosci.* **11**, 621–625 (1995).
29. Klein, R. G. *The Human Career: Human Biological and Cultural Origins* (Univ. Chicago Press, Chicago, 1989).
30. Reider, M. J., Taylor, S. L., Tobe, V. O. & Nickerson, D. A. Automating the identification of DNA variations using quality-based fluorescence re-sequencing: analysis of the human mitochondrial genome. *Nucleic Acids Res.* **26**, 967–973 (1998).

**Acknowledgements**

We thank M. Stoneking for his advice regarding the analysis of recombination, and L. Cavalli-Sforza, G. Destro-Bisol, L. Excoffier, T. Jenkins, K. Kidd, J. Kidd, G. Klein, R. Mahabeer, V. Nasidze, E. Poloni, H. Soodyall, M. Stoneking, M. Voevoda and S. Wells for samples. This work was supported by grants from Swedish Natural Sciences Research Council and Beijer Foundation.

Correspondence and requests for materials should be addressed to U.G. (e-mail: ulf.gyllensten@genpat.uu.se).

**The HIC signalling pathway links CO<sub>2</sub> perception to stomatal development**

**Julie E. Gray\***, **Geoff H. Holroyd†**, **Frederique M. van der Lee‡**, **Ahmad R. Bahrami\***, **Peter C. Sijmons§**, **F. Ian Woodward||**, **Wolfgang Schuch¶** & **Alistair M. Hetherington†**

\* Department of Molecular Biology and Biotechnology, University of Sheffield, Sheffield S10 2TN, UK

† Department of Biological Sciences, University of Lancaster, Lancaster LA1 4YQ, UK

‡ Zeneca Mogen, PO Box 628, 2300 AP Leiden, The Netherlands

§ Cellscreen, PO Box 134, 6700 AC Wageningen, Netherlands

|| Department of Animal and Plant Sciences, University of Sheffield, Sheffield, S10 2TN, UK

¶ Zeneca Wheat Improvement Centre, Norwich Research Park, Colney, Norwich NR4 7UH, UK

Stomatal pores on the leaf surface control both the uptake of CO<sub>2</sub> for photosynthesis and the loss of water during transpiration. Since the industrial revolution, decreases in stomatal numbers in parallel with increases in atmospheric CO<sub>2</sub> concentration have provided evidence of plant responses to changes in CO<sub>2</sub> levels caused by human activity<sup>1,2</sup>. This inverse correlation between stomatal density and CO<sub>2</sub> concentration also holds for fossil material from the past 400 million years<sup>3</sup> and has provided clues to the causes of global extinction events<sup>4</sup>. Here we report the

identification of the *Arabidopsis* gene *HIC* (for high carbon dioxide), which encodes a negative regulator of stomatal development that responds to CO<sub>2</sub> concentration. This gene encodes a putative 3-keto acyl coenzyme A synthase—an enzyme involved in the synthesis of very-long-chain fatty acids<sup>5</sup>. Mutant *hic* plants exhibit up to a 42% increase in stomatal density in response to a doubling of CO<sub>2</sub>. Our results identify a gene involved in the signal transduction pathway responsible for controlling stomatal numbers at elevated CO<sub>2</sub>.

As part of a promoter trap screen aimed at isolating tissue-specific genes in *Arabidopsis thaliana*<sup>6,7</sup>, we identified an individual plant designated *hic* in which the  $\beta$ -glucuronidase (*GUS*) reporter gene was expressed only in the guard cells (Fig. 1) and nowhere else in the plant. Southern analysis of *hic* genomic DNA using a *GUS* gene probe detected a single band, suggesting that there was only one *GUS* gene insertion in this line (data not shown).

We next investigated the phenotype of the *hic* mutant and found it to be different from previously described *Arabidopsis* stomatal development mutants<sup>8,9</sup>. *hic* stomata had no obvious phenotype and the plants were not wilting, suggesting that guard-cell function was not impaired. *hic* guard cells increased turgor in response to light and reduced turgor in response to the addition of the plant hormone abscisic acid in stomatal bioassays (data not shown). *hic* plants were indistinguishable from the parental ecotype when analysed by infrared thermography (data not shown); however, analysis of plants that had been grown under differing CO<sub>2</sub> concentrations showed that the *HIC* gene affects stomatal development.

We grew *hic* and C24, the parental ecotype, at elevated and ambient concentrations of CO<sub>2</sub>, and measured the stomatal index and density on the leaf surface. A reduction in stomatal index and density in response to elevated CO<sub>2</sub> is well characterized in some species, including three ecotypes of *Arabidopsis*<sup>1,2</sup>, and indicates that the plant has the potential for increased water-use efficiency with increasing CO<sub>2</sub>. Table 1 shows that growth of *hic* plants under elevated CO<sub>2</sub> induced marked increases in both stomatal index and

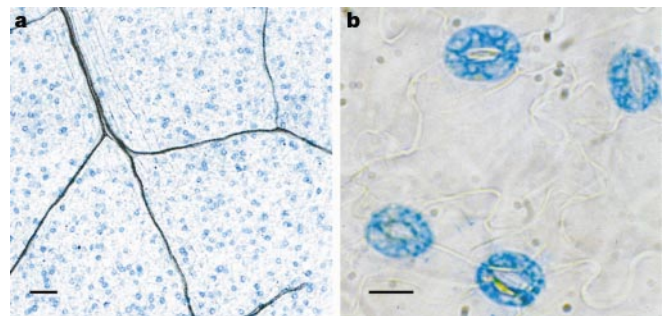


**Figure 1** *GUS* expression in *hic Arabidopsis* plants is specific to guard cells. Part of a *hic* leaf histochemically stained for *GUS* activity shows guard-cell-specific expression at low (a; scale bar, 100  $\mu$ m) and higher magnification (b; scale bar, 10  $\mu$ m).

**Table 1** Effect of ambient and elevated CO<sub>2</sub> on stomatal and epidermal cell density and stomatal index

Experiment	Line	Stomatal density (n mm <sup>-2</sup> )				Epidermal cell density (n mm <sup>-2</sup> )				Stomatal index (%)			
		Ambient	Elevated	Difference (P)	% change	Ambient	Elevated	Difference (P)	% change	Ambient	Elevated	Difference (P)	% change
1	C24	280 (9)	233 (8)	<0.001	-17.0	1,047 (9)	902 (8)	<0.001	-13.8	21.1 (9)	20.5 (8)	NS	-3.1
	<i>hic</i>	231 (8)	320 (8)	<0.001	+38.0	891 (8)	902 (8)	NS	+1.2	20.8 (8)	26.0 (8)	<0.005	+25
2	C24	265 (7)	245 (9)	NS	-7.8	1,056 (7)	1,028 (9)	NS	-2.7	20.0 (7)	19.1 (9)	NS	-4.4
	<i>hic</i>	257 (9)	324 (10)	<0.001	+25.2	1,047 (9)	1,061 (10)	NS	+1.3	19.8 (9)	23.2 (10)	<0.001	+17.8
3	C24	324 (9)	245 (7)	<0.001	-24.5	1,322 (9)	1,058 (7)	<0.005	-20	19.6 (9)	18.7 (7)	NS	-4.7
	<i>hic</i>	273 (7)	387 (9)	<0.001	+41.8	1,053 (7)	1,092 (9)	NS	+3.7	20.5 (7)	26.2 (9)	<0.001	+27.6
4	C24	273 (12)	283 (12)	NS	+3.1	1,052 (12)	1,049 (12)	NS	-0.3	20.6 (12)	21.2 (12)	NS	+3.2
	<i>hic</i>	266 (12)	351 (12)	<0.001	+31.8	1,035 (12)	1,062 (12)	NS	+2.6	20.6 (12)	24.9 (12)	<0.001	+21.2

Data are presented for four separate experiments in the *hic* mutant and the parental ecotype (C24). The average density or stomatal index is presented for each treatment. The numbers in brackets indicate the number of individual plants in each treatment. Treatments were compared using the Mann-Whitney Rank Sum Test (SigmaStat 2.03). NS, not significant.

density. By contrast, CO<sub>2</sub> enrichment induced no significant changes in stomatal index and either reductions or no significant change in stomatal density of the C24 control plants. Although the C24 ecotype of *Arabidopsis* appears relatively insensitive to CO<sub>2</sub>, other ecotypes of this species show reductions in stomatal density in response to elevated CO<sub>2</sub> (ref. 2). These data suggested that the *HIC* gene product is involved in a signal transduction pathway in which elevated CO<sub>2</sub> influences stomatal development.

To confirm that the disruption of *HIC* was responsible for the increase in stomatal index observed at elevated CO<sub>2</sub>, we adopted two independent experimental procedures. First, we showed that the *GUS* insertion in *hic* plants co-segregated with the increased stomatal index phenotype when these plants were grown at elevated CO<sub>2</sub>. T2 generation *hic* seeds (from a seed population that segregated 3:1 on selective media) were germinated without selection and the plants were grown under elevated CO<sub>2</sub>. A leaf that had developed during growth at elevated CO<sub>2</sub> was removed from each plant and scored for stomatal index and the presence of the *GUS* gene was determined for each plant using polymerase chain reaction (PCR) and a histochemical *GUS* assay. All plants containing the *GUS* transgene had *GUS* activity and had significantly higher stomatal indices than those that lacked this insert (Fig. 2). *HIC* does not act as a recessive gene, and these results are consistent with a dominant-negative or gene-dosage effect.

Second, we tried to replicate the *hic* phenotype by manipulating the expression of the *HIC* gene. We transformed the C24 ecotype with a gene construct designed to express antisense *HIC* mRNA (see below for complementary DNA identification). When three independently transformed lines of T3 generation antisense plants were

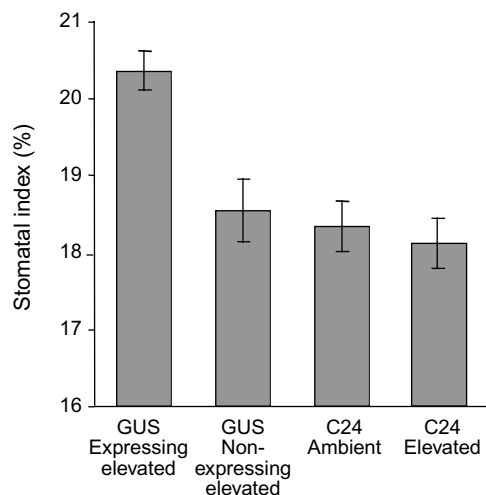


**Figure 2** The *GUS* gene co-segregates with the elevated CO<sub>2</sub> stomatal index phenotype. T2 *hic* seeds were germinated on non-selective media before transfer to the elevated CO<sub>2</sub> chamber for 22 days. Of the 20 plants, 16 showed *GUS* expression and 4 did not, on the basis of a histochemical *GUS* assay<sup>22,23</sup>. Bars represent standard error.  $P < 0.001$  between *GUS* expressers and *GUS* non-expressers. A similar set of data was obtained in a second, separate run of this experiment (not shown).

grown under elevated CO<sub>2</sub>, they all showed significant increases in stomatal index (Table 2). PCR with reverse transcription of RNA (RT-PCR) indicated that these antisense lines had reduced levels of *HIC* messenger RNA (see Methods). The results from this experiment show that when the expression of *HIC* is reduced plants have increased stomatal index and density at elevated CO<sub>2</sub>. Both these results provide strong support for our hypothesis that the increase in stomatal index observed when *hic* plants are grown at elevated CO<sub>2</sub> is caused by a disruption in *HIC*.

To study the nature of the *HIC* gene, we isolated a region of DNA from the *hic* genome adjacent to the inserted *GUS* gene. This *hic* DNA fragment was used to identify genomic and cDNA *HIC* gene fragments from non-tagged *Arabidopsis*. Analysis of the nucleotide sequences showed that the *GUS* gene had inserted in *hic* plants slightly downstream from a predicted open reading frame in the 3' untranslated region of a transcribed gene. It was also apparent that the *HIC* gene was disrupted by a fragment of mitochondrial DNA introducing three stop codons. This would be expected to result in the production of a severely truncated gene product (Fig. 3). On the basis of nucleotide and derived peptide sequence homologies, *HIC* was found to be most similar to the *Arabidopsis KCS1* gene that encodes a 3-ketoacyl coenzyme A (CoA) synthase<sup>10</sup> (KCS; Fig. 3). As the insertion of the fragment of mitochondrial DNA into the *HIC* gene is expected to terminate translation in the predicted active site of the KCS enzyme<sup>11</sup> (Fig. 3), it seems likely that the activity of the *HIC*-encoded putative KCS will be considerably reduced.

Our data indicate that the activity of a guard-cell KCS, the condensing enzyme in the microsomal fatty-acid elongase complex<sup>10</sup>, may be involved in the stomatal patterning response to elevated CO<sub>2</sub>. Fatty-acid elongases catalyse the synthesis of very long chain fatty acids, and in plants they are involved in the synthesis of waxes, glycerolipids, sphingolipids and cutin<sup>5</sup>. In *hic* plants, it is possible that the lesion in this putative KCS prevents the synthesis of component(s) of the extracellular matrix found at the guard-cell surface. Our hypothesis to account for the *hic* phenotype is that loss of the component(s) synthesized by *HIC* results in a modification of stomatal development in response to CO<sub>2</sub>.

Other, independent evidence lends support to our hypothesis. We reasoned that as *HIC* encodes a putative KCS and KCS enzymes are involved in wax biosynthesis, plants carrying lesions in wax biosynthesis genes should display aberrant stomatal densities when compared with wild-type plants. In fact, almost 30 years ago, the barley wax-deficient *eceriferum-g* mutant was reported to display abnormal stomatal patterning<sup>12</sup>. We examined stomatal indices in the *cer1* and *cer6* wax-accumulation mutants of *Arabidopsis*<sup>13,14</sup>. With respect to their parental ecotype, both *cer1* and *cer6* displayed greatly increased stomatal indices (Table 3). These results show that alterations in leaf wax biosynthesis in *Arabidopsis* are associated with aberrant stomatal densities, in support of our hypothesis. In the case of *hic*, however, the disruption to wax biosynthesis must be subtle, as a scanning electron microscopic comparison of the epidermis of *hic* and C24 revealed no obvious differences in wax morphology (data not shown).

The link between the putative guard-cell KCS gene *HIC* and alterations in stomatal density is supported by work on another

**Table 2** Effect of ambient and elevated CO<sub>2</sub> on stomatal and epidermal cell densities and stomatal indices

Line	Stomatal density (n mm <sup>-2</sup> )				Epidermal cell density (n mm <sup>-2</sup> )				Stomatal index (%)			
	Ambient	Elevated	Difference (P)	% change	Ambient	Elevated	Difference (P)	% change	Ambient	Elevated	Difference (P)	% change
C24	242 (9)	252 (11)	NS	+4.1	990 (9)	1,088 (11)	NS	+9.9	19.6 (9)	18.8 (11)	NS	-4.2
Antisense 1	235 (9)	286 (10)	<0.001	+21.7	1,028 (9)	1,062 (10)	NS	+3.3	18.6 (9)	21.2 (10)	<0.001	+13.9
Antisense 2	240 (10)	272 (10)	<0.001	+13.3	1,010 (10)	997 (10)	NS	-1.3	19.2 (10)	21.5 (10)	<0.001	+11.9
Antisense 3	243 (10)	263 (9)	<0.03	+8.2	929 (10)	907 (9)	NS	-2.4	20.7 (10)	22.5 (9)	<0.001	+8.7

Comparisons between *Arabidopsis* plants transformed with the *HIC* gene in an antisense orientation and the C24 ecotype were done by the Mann-Whitney Rank Sum Test (SigmaStat 2.03). NS, not significant.

*Arabidopsis* KCS gene called *FIDDLEHEAD* (*FDH*) (Fig. 3). Mutations in *FDH* manifest themselves in a range of developmental responses<sup>15,16</sup>, however, from the perspective of our results, the most interesting observation is that mutations in *FDH* alter leaf epidermal cell fate and specifically control trichome development<sup>17</sup>. Given that trichomes and guard cells both develop from proto-dermal cells<sup>18</sup>, this is very strong evidence that the product(s) of KCS enzymes are capable of altering the fate of cells in the leaf epidermis.

Our results indicate that *hic* plants carry a mutation in a KCS gene that results in a disruption in the signal transduction pathway responsible for the control of stomatal patterning in response to elevated CO<sub>2</sub>. The simplest explanation, consistent with existing data on KCS<sup>16</sup>, to account for the *hic* phenotype is that disruption of the putative KCS encoded by *HIC* results in altered permeability of the guard-cell extracellular matrix. These alterations in guard-cell extracellular matrix permeability then alter the diffusion of an elevated CO<sub>2</sub>-stimulated morphogen responsible for the control of stomatal development. As the normal response to elevated CO<sub>2</sub> is either to reduce stomatal index and density or to keep them unchanged (Table 1), it seems likely that this morphogen is a negative regulator of guard-cell development. These results are in line with the lateral inhibition hypothesis for the control of stomatal development<sup>19,20</sup> and are consistent with current ideas on the role of cell-cell communication in stomatal patterning<sup>18</sup>. To our knowledge, *HIC* is the first gene to be identified that affects the developmental responses of plants to global changes in atmospheric composition. □

### Methods

#### Plant material and growth conditions

We used the following plant material: *hic*, *cer1*, *cer6* (refs 13, 14) and ecotypes. Vernalized seeds were germinated on 0.5× Murashige and Skoog basal salts, 1% (w/v) sucrose, 0.6% (w/v) agar at 22–24 °C under a 10 h/14 h light (150 μmol m<sup>-2</sup> s<sup>-1</sup>)/ dark regime. Where selection was required, media included 10 mg l<sup>-1</sup> hygromycin. To investigate the effects of elevated CO<sub>2</sub>, resistant plants were selected from a non-homozygous T2 *hic* line (segregating roughly 3:1 resistant:susceptible on hygromycin) and transferred to a peat-based compost mix at 16–18 days old. *C24* and *hic* plants were then grown in a matched pair of chambers built using the hot gas bypass system as described<sup>21</sup> for 22–27 days at 22 °C ± 0.5 day, 22 °C ± 0.5 night, 10 h/14 h light/dark regime, 60% relative humidity, 180 μmol m<sup>-2</sup> s<sup>-1</sup> lighting. CO<sub>2</sub> concentration was controlled (elevated 1,000 p.p.m. ± 100 and ambient 350–480 p.p.m.) and monitored by an infrared gas analyser (WMA-2, PP Systems) switched between chambers by a solenoid valve on a 30-s cycle.

#### GUS staining

Leaves were histochemically stained for the presence of the GUS gene product as described<sup>22</sup> followed by a clearing step<sup>23</sup>.

#### Determination of stomatal indices

A leaf that had developed during the course of the experiment was removed from each plant and stomatal density, epidermal density and stomatal index determined as described<sup>24</sup> from the abaxial surface of three areas of each leaf using the dental rubber impression technique<sup>25,26</sup>. Leaves were selected on the basis of uniform comparable size between treatments and across experiments.

#### Analysis of the *HIC* gene sequence

*hic* DNA 5' to the *GUS* gene insertion was isolated by inverse PCR essentially as described<sup>27</sup> using *pfu* polymerase, oligonucleotide primers 5'-CAGAACTTACGTACACTTTTC-3' and 5'-CATCTTCTCTATGCCACTACT-3', and *EcoRV*-restricted *hic* genomic DNA, and ligated into pGEMT (Promega) to produce pFL44. This was used as a probe to screen a



**Figure 3** *HIC* is similar to *Arabidopsis* 3-keto acyl CoA synthases. Alignment of the predicted peptide sequence of *HIC* with those of KCS<sup>10</sup> (accession number AF053345) and FDH<sup>15–17</sup> (accession number AJ010713) with identical residues highlighted in black

and the tentatively identified active-site cysteine<sup>11</sup> marked with an asterisk. The arrow indicates the position of the mitochondrial DNA insertion that disrupts the *HIC* gene in the region of the putative active site.

**Table 3** Stomatal indices of *cer1* and *cer6* *eceriferum* mutants of *Arabidopsis* and their parental ecotype

Genetic background	Stomatal index (%)	Difference (P)	Relative % change
Ler	11.8 (8)	–	–
<i>cer1</i>	16.9 (7)	<0.005	+43.2
<i>cer6</i>	15.4 (15)	<0.005	+30.5

The numbers in brackets indicate the number of plants examined. Comparison with parental ecotype, *landsberg erecta* (Ler) was made using Student's *t*-test.



C24 *Arabidopsis* genomic DNA library and isolate a *Bgl*II genomic DNA fragment encoding the complete *HIC* open reading frame, and also to identify ATTS5501 expressed sequence tag (clone YAY1019) by a BLASTN homology search of the dbest database (this cDNA was provided by J. Giraudat, CNRS, Gif, France). The complete nucleotide sequences of ATTS5501 (2,073 bp), pFL30 (5,600 bp) and pFL44 (1,584 bp) inserts were determined. The *HIC* gene is identical to a region of BAC T3A4 (accession no. AC005819) on *Arabidopsis* chromosome 2. The cloned sequences pFL30 and ATTS5501 are identical in their regions of overlap. pFL44 contains an additional 123-bp mitochondrial DNA insertion from nucleotide position 482–604 (identical to part of the *Arabidopsis* mitochondrial genome sequence part B (accession number Y08502) which is also present elsewhere on chromosome 2; ref. 28). It is probable that the insertion causing the *hic* mutation occurred during the *Agrobacterium-tumefaciens*-mediated transformation process used to generate *hic*. PCR was used to confirm the presence of this mitochondrial DNA insertion in *hic* plants and its absence in C24. The *GUS* gene is inserted 89-bp 3' of the putative *HIC* stop codon. RT-PCR was used to confirm the presence of the *GUS* insert downstream of *hic* in the same gene transcript by amplifying a fragment of DNA that spanned the two coding regions.

## Generation of *HIC* antisense plants.

ATTS5501 cDNA was excised from pBluescript using *Eco*RI and ligated into pART7 (ref. 29). The resulting plasmid was digested with *Nof*I to release the cDNA in the reverse orientation between the CaMV 35S RNA promoter and OCS 3' terminator which was ligated into pART27 (ref. 29). Gene constructs were confirmed by DNA sequencing and *Agrobacterium*-mediated transformation was carried out as described<sup>30</sup>. The presence of the transgene in plants was verified by PCR (data not shown). RT-PCR with primers (5'-GCTAGTGGTGAACGTCATGC-3' and 5'-ACAAAATCGTTACCGCAAG-3' designed specifically to amplify a 1,281-bp region of the 5' untranslated portion of the *HIC* mRNA that differs from other known *KCS*-like genes) was used to show that the level of the *HIC* gene transcript was either considerably reduced in the antisense plants (line AS3) or undetectable by this method (AS1 and AS2), in comparison with C24 plants, which gave a clear band of DNA of the expected size on agarose gel electrophoresis. Separate amplification reactions with ubiquitin-specific primers were carried out to confirm equal amounts of mRNA. Control reactions minus reverse transcriptase gave no signal.

Received 15 May; accepted 23 October 2000.

- Woodward, F. I. Stomatal numbers are sensitive to CO<sub>2</sub> increases from pre-industrial levels. *Nature* **327**, 617–618 (1987).
- Woodward, F. I. & Kelly, C. K. The influence of CO<sub>2</sub> concentration on stomatal density. *New Phytol.* **131**, 311–327 (1995).
- McElwain, J. C. & Chaloner, W. G. Stomatal density and index of fossil plants track atmospheric carbon-dioxide in the paleozoic. *Ann. Bot.* **76**, 389–395 (1995).
- McElwain, J. C., Beerling, D. J. & Woodward, F. I. Fossil plants and global warming at the Triassic–Jurassic boundary. *Science* **285**, 1386–1390 (1999).
- Post-Beittenmiller, D. Biochemistry and molecular biology of wax production in plants. *Annu. Rev. Plant Physiol. Plant Mol. Biol.* **47**, 405–430 (1996).
- Topping, J. F., Wei, W. B. & Lindsey, K. Functional tagging of regulatory elements in the plant genome. *Development* **112**, 1009–1019 (1991).
- Goddijn, O. J. M., Lindsey, K., van der Lee, F. M., Klap, J. C. & Sijmons, P. C. Differential gene-expression in nematode-induced feeding structures of transgenic plants harbouring GUSA fusion constructs. *Plant J.* **4**, 863–873 (1993).
- Yang, M. & Sack, F. D. The *too many mouths* and *four lips* mutations affect stomatal production in *Arabidopsis*. *Plant Cell* **7**, 2227–2239 (1995).
- Berger, D. & Altman, T. A subtilisin-like serine protease involved in the regulation of stomatal density and distribution in *Arabidopsis thaliana*. *Genes Dev.* **14**, 1119–1131 (2000).
- Todd, J., Post-Beittenmiller, D. & Jaworski, J. G. *KCSI* encodes a fatty acid elongase 3-ketoacyl-CoA synthase affecting wax biosynthesis in *Arabidopsis thaliana*. *Plant J.* **17**, 119–130 (1999).
- Lassner, M. W., Lardizabal, K. & Metz, J. G. A jojoba β-keto-CoA synthase cDNA complements the canola fatty acid elongation mutation in transgenic plants. *Plant Cell* **8**, 281–292 (1996).
- Zeyher, E. & Stebbins, L. Developmental genetics in barley: a mutant for stomatal development. *Am. J. Bot.* **59**, 143–148 (1972).
- Jenks, M. A., Tuttle, H. A., Eigenbrode, S. D. & Feldmann, K. A. Leaf epicuticular waxes of the *ecriterium* mutants in *Arabidopsis*. *Plant Physiol.* **108**, 369–377 (1995).
- Post-Beittenmiller, D. The cloned *Ecriterium* genes of *Arabidopsis* and the corresponding *Glossy* genes in maize. *Plant Physiol. Bioch.* **36**, 157–166 (1998).
- Lolle, S. J., Cheung, A. Y. & Sussex, I. M. *fiddlehead*: an *Arabidopsis* mutant constitutively expressing an organ fusion program that involves interactions between epidermal cells. *Dev. Biol.* **152**, 383–392 (1992).
- Lolle, S. J. *et al.* Developmental regulation of cell interactions in the *Arabidopsis fiddlehead-1* mutant: a role for the epidermal cell wall and cuticle. *Dev. Biol.* **189**, 311–321 (1997).
- Yephremov, A. *et al.* Characterization of the *FIDDLEHEAD* gene of *Arabidopsis* reveals a link between adhesion response and cell differentiation in the epidermis. *Plant Cell* **11**, 2187–2201 (1999).
- Larkin, J. C., Marks, M. D., Nadeau, J. & Sack, F. Epidermal cell fate and patterning in leaves. *Plant Cell* **9**, 1109–1120 (1997).
- Bünning, E. & Sagromsky, H. Die Bildung des Spaltöffnungsmusters in der Blattepidermis. *Z. Naturforsch.* **3b**, 203–216 (1948).
- Korn, R. W. Evidence in dicots for stomatal patterning by inhibition. *Int. J. Plant Sci.* **154**, 367–377 (1993).
- Neighbour, E. A. *et al.* A small-scale controlled environment chamber for the investigation of effects of pollutant gases on plants growing at cool or sub-zero temperature. *Environ. Pollution* **64**, 155–168 (1990).
- Jefferson, R. A. Assaying chimeric genes in plants: The *GUS* gene fusion system. *Plant Mol. Biol. Rep.* **5**, 387–405 (1987).
- Beckman, A. A. & Engler, A. A. An easy technique for the clearing of histochemically stained plant tissue. *Plant Mol. Biol. Rep.* **12**, 37–42 (1994).

- Salisbury, E. J. On the causes and ecological significance of stomatal frequency with special reference to woodland flora. *Phil. Trans. R. Soc. Lond. B* **216**, 1–65 (1927).
- Weyers, J. D. B. & Johansen, L. G. Accurate estimation of stomatal aperture from silicone rubber impressions. *New Phytol.* **101**, 109–115 (1985).
- Poole, L., Weyers, J. D. B., Lawson, T. & Raven, J. A. Variations in stomatal density and index: implications for paleoclimatic reconstructions. *Plant Cell Environ.* **19**, 705–712 (1996).
- Barthels, N. *et al.* Regulatory sequences of *Arabidopsis* drive reporter gene expression on nematode feeding structures. *Plant Cell* **9**, 2119–2134 (1997).
- Lin, X. Y. *et al.* Sequence and analysis of chromosome 2 of the plant *Arabidopsis thaliana*. *Nature* **402**, 761–765 (1999).
- Gleave, A. P. A versatile binary vector system with a T-DNA organisational structure conducive to efficient integration of cloned DNA into the plant genome. *Plant Mol. Biol.* **20**, 1203–1207 (1992).
- Valvekens, D., Van Montagu, M. & Van Lijsebettens, M. *Agrobacterium tumefaciens*-mediated transformation of *Arabidopsis thaliana* root explants by using kanamycin selection. *Proc. Natl Acad. Sci. USA* **85**, 5536–5540 (1988).

## Acknowledgements

We acknowledge the assistance of J. Proctor, J. Balk, A. G. Moir and P. Tripathi with this work. We would like to thank K. Lindsey and S. Bright for helpful discussions.

Correspondence and requests for materials should be addressed to A.M.H. (e-mail: A.Hetherington@lancaster.ac.uk). The accession numbers for ATTS 5501, FL30 and FL44 are in GenBank under accession numbers AF188484, AF188485 and AF188486, respectively.

# The *ELF3 zeitnehmer* regulates light signalling to the circadian clock

Harriet G. McWatters\*, Ruth M. Bastow\*, Anthony Hall & Andrew J. Millar

Department of Biological Sciences, University of Warwick, Gibbet Hill Road, Coventry, CV4 7AL, UK

\* These authors contributed equally to this work

The circadian system regulates 24-hour biological rhythms<sup>1</sup> and seasonal rhythms, such as flowering<sup>2</sup>. Long-day flowering plants like *Arabidopsis thaliana*, measure day length with a rhythm that is not reset at lights-off<sup>3</sup>, whereas short-day plants measure night length on the basis of circadian rhythm of light sensitivity that is set from dusk<sup>2</sup>. *early flowering 3 (elf3)* mutants of *Arabidopsis* are photoperiodic<sup>4</sup> and exhibit light-conditional arrhythmia<sup>5,6</sup>. Here we show that the *elf3-7* mutant retains oscillator function in the light but blunts circadian gating of *CAB* gene activation, indicating that deregulated phototransduction may mask rhythmicity. Furthermore, *elf3* mutations confer the resetting pattern of short-day photoperiodism, indicating that gating of phototransduction may control resetting. Temperature entrainment can bypass the requirement for normal *ELF3* function for the oscillator and partially restore rhythmic *CAB* expression. Therefore, *ELF3* specifically affects light input to the oscillator, similar to its function in gating *CAB* activation, allowing oscillator progression past a light-sensitive phase in the subjective evening. *ELF3* provides experimental demonstration of the *zeitnehmer* ('time-taker') concept<sup>7,8</sup>.

As *elf3* mutants are rhythmic in darkness (DD)<sup>5,6</sup>, *ELF3* cannot be an essential component of the circadian oscillator. We tested whether the apparent arrhythmia in constant light (LL) of *elf3* plants was in fact masking an underlying oscillation. We entrained wild-type, null mutant *elf3-1* and partial mutant *elf3-7* (refs 5, 6) plants to light/dark cycles (LD), transferred them to LL and released replicate samples into DD at 2-h intervals, monitoring the phase of *CAB* expression in DD to determine the state of the oscillator in the preceding LL interval. We reasoned that if an underlying oscillator in the *elf3* mutants was masked by constant illumination, its phase should be reflected in the phase of the peak in DD. If the oscillator were dysfunctional in *elf3* mutants under LL, the timing of the *CAB*